

Measuring the (Un)Faithfulness of Concept-Based Explanations

Shubham Kumar
UIUC
s1138@illinois.edu

Narendra Ahuja
UIUC
n-ahuja@illinois.edu

Abstract

*Post-hoc, unsupervised concept-based explanation methods (U-CBEMs) translate a vision model’s internal reasoning into human-understandable concepts, leading to interpretable explanations. However, we find that many state-of-the-art (SOTA) U-CBEMs are **not faithful**: their concepts seem interpretable but fail to reproduce the model’s predictions. We argue that this deficiency has gone unnoticed due to fragmented evaluation—each paper proposes its own faithfulness measure, with no measure-over-measure comparison or broad benchmarking. We close this gap by (i) organizing prior metrics in a unified framework, discussing their limitations, and identifying desiderata for a faithfulness measure; (ii) introducing the **Surrogate Faithfulness (SURF) measure**, which quantifies faithfulness via the predictive loss of a surrogate that maps explanations to the model’s outputs; and (iii) delivering the first comprehensive U-CBEM faithfulness benchmark across diverse tasks and architectures. In a controlled setting, SURF outperforms prior faithfulness measures in measure-over-measure comparisons, and applying SURF to SOTA U-CBEMs reveals that many visually appealing U-CBEMs are surprisingly unfaithful. We demonstrate SURF applicability in two downstream settings—(i) faithfulness versus the number of concepts used in the explanation and (ii) U-CBEM robustness to adversarial attacks—underscoring SURF’s value as a reliable faithfulness measure. Code to be released.*

1. Introduction

Deep learning models have delivered state-of-the-art results across diverse tasks, yet their internal reasoning remain difficult to interpret [12], which is especially problematic in high-stakes domains such as healthcare and finance. This gap has given rise to explainable AI (XAI), whose goal is to produce *explanations* of model behavior. Two properties characterize explanation quality: *interpretability*—explanations that humans can understand—and *faithfulness*—explanations that accurately reflect the model’s internal reasoning and allow humans to reliably predict the

model’s output. XAI methods must balance the natural tension between interpretability and faithfulness. While interpretability is typically assessed with human studies, faithfulness can be evaluated by defining a *surrogate* that maps the explanation to the model’s outputs and measuring the loss between the surrogate and model. Because explanations are inevitably lossy, some discrepancy between the surrogate and the model is expected; a faithfulness measure must therefore specify both (i) an appropriate surrogate and (ii) a metric for the induced loss.

One broad family of XAI methods constructs *inherently interpretable models*, injecting an explanatory structure directly into the model. Since the explanation and the model are merged, these approaches eliminate the need for faithfulness checks; however, they often underperform blackbox models by reducing model complexity (capacity) for explainability. In contrast, *feature attribution* methods express a trained model’s outputs in terms of each input feature’s contribution—commonly found through gradients or perturbations [7, 23, 28, 30, 38]. For images, these attributions are visualized as pixel-level heatmaps. Although such explanations are intuitive, attributions are usually unfaithful, since they are estimated from noisy gradients in deep neural networks or from unrealistic perturbations on the input space [1, 11, 15, 32]. The heatmaps also lack interpretability—they only indicate *where* the model attends, not *what* semantics it recognizes [4, 26].

Concept-based explanation methods (CBEMs) improve interpretability by explaining predictions in terms of human-understandable *concepts* (e.g., edges, colors, object parts) [3, 10, 17, 46]. To recognize concepts, supervised CBEMs require a concept-annotated image dataset, which is costly and subjective; moreover, any fixed concept vocabulary may bias the explanation and miss aspects of the model’s reasoning, raising faithfulness concerns [29]. To avoid annotation, *unsupervised* CBEMs (U-CBEMs) discover concepts automatically as *concept activation vectors* (CAVs)—directions in the model’s intermediate representation space—paired with a *concept importance* score that captures the concept’s relevance to the output.

We argue that, in practice, U-CBEMs have prioritized in-

terpretability at the expense of faithfulness, yielding explanations that look compelling but are surprisingly unfaithful. Despite the importance of faithful explanations, we find that *all prior works introduce new faithfulness measures*, with no measure-over-measure comparison and sparse cross-U-CBEM evaluations. Thus, there is a lack of consensus on faithfulness measures for U-CBEMs, limiting our understanding of how faithful current approaches are.

This work serves to address this gap. Our contributions are to:

1. **Organize prior U-CBEM faithfulness measures** under a common framework, allowing us to discuss limitations in current measures and identify appropriate desiderata for a faithfulness measure.
2. **Propose Surrogate Faithfulness (SURF)**, a faithfulness measure satisfying the desiderata. We *conduct a measure-over-measure comparison* to empirically validate our faithfulness measure against prior measures.
3. **Conduct the first, comprehensive faithfulness benchmark of current U-CBEMs** across a variety of tasks and model architectures. Most SOTA U-CBEMs that were thought to be faithful are found not to be.
4. **Extend SURF to two downstream applications.** First, studying *faithfulness as a function of the number of concepts* shows that some U-CBEMs do not get more faithful as they discover more concepts. Second, analyzing the faithfulness of U-CBEMs when *the model is under adversarial attack* reveals robustness issues.

2. Preliminaries

We first introduce notation that will be used in the remainder of the paper, as well as preliminaries to familiarize the reader with the field.

Background: Model $\phi : \mathcal{X} \rightarrow \mathcal{Y}$ maps from an input space $\mathcal{X} \subseteq \mathbb{R}^P$ to an output space $\mathcal{Y} \subseteq \mathbb{R}^C$. Assume ϕ admits an intermediate space $\mathcal{H} \subseteq \mathbb{R}^D$. Let $g : \mathcal{X} \rightarrow \mathcal{H}$ and $f : \mathcal{H} \rightarrow \mathcal{Y}$. Thus, $\phi(\mathbf{X}) = f(g(\mathbf{X}))$. Let $g(\mathbf{x}) = \mathbf{h} \in \mathcal{H}$ represent the embedding of \mathbf{x} (e.g., image patch), and $g(\mathbf{X}) = \mathbf{H} \in \mathbb{R}^{(HW) \times D}$ denotes the vectorized application of g on $\mathbf{X} = [\mathbf{x}_1 \ \cdots \ \mathbf{x}_{HW}]^T$, where H, W are the spatial dimensions.

Let E be an explanation function, and let $\mathbf{e} = E(\mathbf{X}) \in \mathcal{E}$ represent the explanation for an $\mathbf{X} \in \mathcal{X}$ (e.g., image). Let $s : \mathcal{E} \rightarrow \mathcal{Y}$ be a surrogate. Motivated by Ribeiro et al. [30], E is completely faithful to ϕ if s reproduces $\phi(\mathbf{X}) \forall \mathbf{X} \in \mathcal{X}$. Thus, a faithfulness measure is defined by a choice of surrogate $s(\cdot)$ and metric $d(\cdot)$ as:

$$Faith(E; d, s) = \int_{\mathcal{X}} d(\phi(\mathbf{X}), s(E(\mathbf{X}))) d\mathbf{X} \quad (1)$$

U-CBEMs: To generate explanations, U-CBEMs find, for all outputs $i \in C$, a set of K CAVs $V_i = \{\mathbf{v}_{i,k}\}_{k=1}^K$ and

their concept importances $A_i = \{\alpha_{i,k}\}_{k=1}^K$. Note that while K can vary per output, all prior works find the same number of CAVs for each output. U-CBEMs also define a mechanism $\mathcal{P}(\mathbf{h}; V) : \mathcal{H} \rightarrow \mathbb{R}^K$ to project embedding \mathbf{h} to the concept space defined by CAVs in V . The explanation for output i is:

$$\begin{aligned} E_i(\mathbf{X}) &= E_i(\mathbf{X}; g, V_i, A_i, \mathcal{P}) \\ &= \{\mathcal{P}(g(\mathbf{X}); V_i), A_i\} \end{aligned} \quad (2)$$

$E_i(\mathbf{X})$ is then conveyed to the user through some visual interface. Note that $\mathcal{P}(g(\mathbf{X}))$ denotes the vectorized application of \mathcal{P} on $g(\mathbf{X}) = \mathbf{H}$.

Following prior works, we study faithfulness in the final layer, where the spatial dimensions $H = W = 1$, so $\mathbf{H} = \mathbf{h}$. Given that U-CBEMs operate on $g(\mathbf{X})$, the faithfulness measure can be simplified to:

$$\begin{aligned} Faith_{U-CBEM}(\mathcal{P}, \{V_i\}_{i=1}^C, \{A_i\}_{i=1}^C; d, s) &= \\ \int_{\mathcal{H}} d(f(\mathbf{h}), \{s(\mathcal{P}(\mathbf{h}; V_i), A_i)\}_{i=1}^C) d\mathbf{h} \end{aligned} \quad (3)$$

3. Related Works

3.1. Unsupervised Concept-Based Explanations

Wang et al. [37] initiated this line of work, finding CAVs by K-Means clustering intermediate embeddings computed on a dataset. Each cluster was associated with a semantic concept (e.g., car tire, window, headlight) by tracing back the clustered embeddings to their corresponding image patches. Ghorbani et al. [13] improve this with ACE, which finds concepts at different scales by hierarchically segmenting images into “candidate” segments and clustering the embeddings of each candidate. To ensure that the discovered CAVs fully represent the model’s behavior, Yeh et al. [39] propose ConceptSHAP (C-SHAP), which finds CAVs that maximize a proposed completeness score; they use Shapley Values [41] to find concept importance. ICE [44] extends ACE by replacing clustering with Non-negative Matrix Factorization (NMF), resulting in a parts-based explanation. The authors show that concepts found with NMF are more interpretable than those found by K-Means or Principal Component Analysis (PCA). Building on this, Fel et al. [9] present CRAFT, which recursively applies NMF through the model to decompose concepts into sub-concepts, and they use sensitivity analysis for finding concept importance. CDISCO [14] uses the singular value decomposition (SVD) to find CAVs and a gradient-based method for finding concept importance. Recently, MCD [35] extends the notion of CAVs to a multidimensional linear subspace, rather than a single vector, allowing it to describe more of the model’s behavior with fewer concepts.

Table 1. **Deletion-Based Measures:** We organize deletion-based measures introduced by prior works according to their differing factors. The factors we use are *Perturbation Space*, *Deletion Strategy*, and how the results are presented (*Y-axis* and *X-axis*). Notice how all prior works introduce a different faithfulness measure, with no measure-over-measure comparison.

Method	Perturbation Space	Deletion Strategy	Y-axis	X-axis
ACE	Pixel	Constant (grey)	Accuracy	# Deleted Concepts
CDISCO (M1)	Pixel	Constant (grey)	# Classes with > 80% accuracy loss	# Deleted Concepts
MCD	Pixel	Inpainting	Accuracy	Fraction of Inpainted Pixels
CRAFT	Concept	Constant (zero)	Change in Class Logit Score	# Deleted Concepts
CDISCO (M2)	Weight	Constant (zero)	Accuracy	# Deleted Concepts

3.2. Concept Bottleneck Models

U-CBEMs are not to be confused with Concept Bottleneck Models (CBMs), which create an inherently explainable concept model meant to replace the original black-box model. These methods [18, 20, 27, 42] train a model to first predict a set of interpretable concepts (e.g., a concept bottleneck); then, they use the concept representation for the task (e.g., object classification). By doing so, CBMs fully decomposes the model’s prediction into interpretable concepts, and exposing the concept representation allows users to intervene (e.g., increase the strength of the “red” concept to help the model recognize the “stop sign”). While CBMs are a promising approach, they typically fail to reach the same performance as black-box models, unless they introduce uninterpretable, “residual” concepts. As CBMs are inherently explainable, the notion of faithfulness does not extend to them. This work will only discuss faithfulness as it pertains to U-CBEMs.

4. Unifying U-CBEM Faithfulness Measures

We provide a comprehensive review of all faithfulness measures that were introduced by the works mentioned in Sec. 3.1. We find that each work uses a *different measure* for faithfulness, indicating a lack of unification in the field and preventing fair comparisons of faithfulness across different U-CBEMs. As part of our unified framework, we place prior faithfulness measures into two categories: 1) deletion-based and 2) surrogate-based. We detail the dimensions across which prior deletion-based measures differ; this is followed by a discussion on their limitations, which raise questions on the validity of past assessments. Then, we similarly characterize prior surrogate-based measures and demonstrate their drawbacks.

4.1. Deletion-Based Measures

Deletion-based measures evaluate faithfulness by observing the effect of deleting a concept on the model’s output. Intuitively, these measures assert that removing the most important concepts will result in the greatest model degradation. After obtaining CAVs and their importances (for a class),

concepts are removed (*Deletion Strategy*) from the input’s *Perturbation Space* in decreasing order of importance, and the effect on the model is measured after each deletion. Results are visualized by plotting the effect on the model (*Y-axis*) with respect to some measure of how many concepts were deleted (*X-axis*). Prior works make different choices along each *italicized dimension* mentioned.

Perturbation Space: defines the space in which concepts are removed. This is either the image space, the model’s weight space, or the concept space. If making removals in the pixel or the weight space, the U-CBEM must have some mechanism to associate the concept to this space (e.g., which pixels in the image represent the concept).

Deletion Strategy: defines how concepts are removed. Concepts are usually removed from the *Perturbation Space* by setting the concept to a baseline value (e.g., 0).

Y-axis: defines what is measured after each deletion. Typically, this is accuracy (e.g., in object classification).

X-axis: represents how much “information” was deleted. This is typically the number of deleted concepts.

To understand the differences between prior deletion measures, Tab. 1 organizes prior measures according to these dimensions. **ACE** [13] deletes concepts in the image space by setting associated pixels to a constant value (Constant Deletion). They measure the model’s prediction accuracy after each deletion across a dataset. **CRAFT** [9] transforms the model’s embeddings into a concept representation. It makes Constant Deletions in the concept space by setting the concept to zero; then, they reconstruct the embedding from the perturbed concept representation. They measure the change in the corresponding class’s logit score. **CDISCO** [14] has two measures. The first measure (M1) makes Constant Deletions in the pixel space and measures the number of classes that have a greater than 80% accuracy degradation. The second measure (M2) deletes concepts by zeroing out parameters in the model’s weight space that are associated with the concept, and they plot classification accuracy. **MCD** [35] deletes concepts in the pixel space by using inpainting. They measure model classification accuracy with respect to the fraction of inpainted pixels, unlike all prior measures that use the number of deleted concepts.

4.1.1. Limitations of Deletion-Based Measures

There are two notable issues with deletion-based metrics that prevent them from accurately evaluating faithfulness. **First, it is unclear how to delete a concept.** Concepts are usually deleted by Constant Deletion, commonly with a baseline of **0**. The baseline must entirely delete the presence of the concept without affecting other concepts. However, the feature attribution literature has shown that common baseline choices do not guarantee that a feature is completely deleted without affecting other features, leading to unfaithful explanations [11]. Removing features by marginalization is more accurate but requires evaluating expensive, high-dimensional expectations.

Second, there are no guarantees that representations in the Perturbation Space will stay on manifold after deletion. The feature attribution literature [2, 11, 33, 34, 40] has found that the perturbed inputs used for creating explanations may be unrealistic, lying off the data manifold. In the off-manifold regions of the data space, a highly nonlinear model behaves unpredictably, so the model’s outputs may not be meaningfully related to input features. Thus, measuring feature importance with off-manifold inputs can lead to incorrect explanations [11]. More seriously, these explanations can be adversarially attacked; in [33], a model’s off-manifold behavior was modified to hide its dependence on undesirable features used for on-manifold inputs. Such issues can be mitigated by generating explanations using on-manifold input perturbations but requires accurate modeling of the input distribution [11, 15, 34, 36, 43].

Deletions in the concept or weight space manipulate intermediate representations, so the same concerns hold. Thus, we argue that deletion metrics have significant unresolved issues that introduce unreliability in their faithfulness evaluations, so we avoid using these approaches.

4.2. Surrogate-Based Measures

Surrogate-based measures evaluate faithfulness by approximating (Eq 3). Any surrogate-based measure must make two choices: 1) what the surrogate s is, and 2) what the metric d is. We will introduce prior faithfulness measures, and then we discuss their limitations.

4.2.1. Desidarata

The faithfulness definition in Eq. (3) does not constrain the surrogate s , but there are certain properties our surrogate should have. *First*, s should be as simple as possible. Recognize that s reflects the mental computation any human interpreter may be expected to do when trying to map the explanation onto the model’s prediction. An interpretable explanation that requires a complex s is effectively useless; it will not give the human interpreter any meaningful insight into how the model reaches its prediction. *Second*,

Table 2. Surrogate-Based Measures: We compare prior surrogate-based measures introduced in ICE and C-SHAP to the proposed Surrogate Faithfulness (SURF) measure. According to our desidarata, we require surrogates that are simple (e.g., not reconstruction-based and not requiring additional parameters), incorporate concept importances into the surrogate, and measure errors across all outputs. Prior works fail to meet these desidarata (except for ICE not requiring additional parameters). We mark in **green** and **red** the properties that meet our desidarata. A **✓** or **✗** denotes that the method does or does not have the property.

Property	ICE	C-SHAP	SURF (Ours)
Reconstruction-Based?	✓	✓	✗
Additional Parameters?	✗	✓	✗
Uses Concept Importance?	✗	✗	✓
Errors on All Outputs?	✗	✗	✓

the s should incorporate all components of the explanation. For example, U-CBEMs explain with both V_i and A_i , so both should be used by the surrogate. If a component is not included, its impact on faithfulness cannot be measured. *Third*, we desire metric(s) d that rewards explanations that can closely reconstruct all model outputs (e.g. across all classes), instead of only the model’s predicted class. This directly follows from Eq. (3).

4.2.2. Prior Surrogate-Based Measures

Prior works have introduced two surrogate-based measures:

ICE-Eval: ICE introduces its own evaluation measure (termed ICE-Eval). ICE-Eval’s surrogate assumes the U-CBEM’s projection operation P has a reconstruction function $\tilde{P}^{-1} : \mathbb{R}^K \rightarrow \mathcal{H}$. Their surrogate then is:

$$s_i(\cdot) = f_i(\tilde{P}^{-1}(P(\mathbf{h}; V_i))) \quad \forall i \quad (4)$$

where $f_i(\cdot)$ denotes the i ’th output from function $f(\cdot)$. ICE-Eval introduces two metrics. Both are only applicable to classification models.

$$ICE_1 = \frac{1}{|\mathcal{V}|} \sum_{\mathbf{x}, t \in \mathcal{V}} \frac{|y_t - \hat{y}_t|}{|y_t|} \quad (5)$$

where t is the index corresponding to the groundtruth class of \mathbf{x} . The second metric is:

$$ICE_2 = \frac{1}{|\mathcal{V}|} \sum_{\mathbf{x} \in \mathcal{V}} \mathbb{1}\{\text{argmax}(\mathbf{p}) = \text{argmax}(\hat{\mathbf{p}})\} \quad (6)$$

C-SHAP-Eval: C-SHAP introduces its own evaluation measure (termed C-SHAP-Eval). Its surrogate learns a two-layer perceptron $\psi_{\text{C-SHAP}} : \mathbb{R}^K \rightarrow \mathcal{H}$:

$$s_i(\cdot) = f_i(\psi_{\text{C-SHAP}}(P(\mathbf{h}; V_i))) \quad \forall i \quad (7)$$

The metric they define is:

$$CSHAP_1 = \frac{\sum_{x,t \in \mathcal{V}} \mathbb{1}\{t = \text{argmax}(\hat{\mathbf{p}})\} - a_r}{\sum_{x,t \in \mathcal{V}} \mathbb{1}\{t = \text{argmax}(\mathbf{p})\} - a_r} \quad (8)$$

where a_r is the accuracy from random predictions.

ICE-Eval and C-SHAP-Eval fail all three of our desiderata. (1) A critical piece of both surrogates is to *reconstruct* the model’s original embedding, and this reconstruction may be non-linear. This step makes the explanation indirectly related to the model’s output, placing a larger burden on the human interpreter. Additionally, C-SHAP introduces learnable parameters via $\psi_{\text{C-SHAP}}$. (2) Neither surrogate depends on concept importances (A'_i s). Thus, unfaithful A_i ’s will *not* alter faithfulness scores. (3) Error is measured with respect to the predicted or groundtruth class, ignoring errors on the remainder of the output distribution.

5. Method: Surrogate Faithfulness (SURF)

Surrogate Faithfulness (SURF) has two components. A simple surrogate maps the explanation to the model’s output (Fig. 1, Step 3); then, outputs from the surrogate and the original model are compared (Fig. 1, Step 4).

5.1. The SURF Surrogate

The final linear layer $\mathbf{F} = [\mathbf{F}_1 \dots \mathbf{F}_C]$ operates on representation \mathbf{H} to give the output $\mathbf{y} \in \mathcal{Y}$. In terms of their components, $\mathbf{H} = [\mathbf{h}_1 \dots \mathbf{h}_{HW}]^T$ and $\mathbf{F}_i = [\mathbf{f}_{i,1} \dots \mathbf{f}_{i,HW}]^T \in \mathbb{R}^{(HW) \times D}$. Thus, output y_i of ϕ is given by:

$$\begin{aligned} y_i &= \sum_{j=1}^{HW} \mathbf{h}_j^T \mathbf{f}_{i,j} = \sum_{j=1}^{HW} \mathbf{h}_j^T \frac{\mathbf{f}_{i,j}}{\|\mathbf{f}_{i,j}\|_2} \|\mathbf{f}_{i,j}\|_2 \\ &\triangleq \sum_{j=1}^{HW} \mathbf{h}_j^T \mathbf{v}_{i,j} \alpha_{i,j} \quad \text{where } \|\mathbf{v}_{i,j}\|_2 = 1 \quad \forall i, j \end{aligned} \quad (9)$$

where $\alpha_{i,j} = \|\mathbf{f}_{i,j}\|_2$. In words, the model’s linear layer projects each embedding \mathbf{h}_j onto a learned, class-specific direction (or *CAV*) $\mathbf{f}_{i,j}$. The projection is scaled by the norm (or *importance*) $\alpha_{i,j}$ of the learned direction. If the model uses global pooling to reduce the final embedding of \mathbf{x} to a single vector, the summation over j above can be omitted.

We define SURF’s surrogate s to take the form of the linear layer (Eq. (9)), where we input the concept basis representation and A_i ’s from any U-CBEM. The surrogate is:

$$\hat{y}_i = \sum_{j=1}^{HW} \sum_{k=1}^K \alpha_{i,k} \mathcal{P}(\mathbf{h}_j; V_i)_k \quad \forall i \quad (10)$$

where $\mathcal{P}(\cdot)_k$ denotes the k ’th element. Following prior U-CBEMs and evaluation measures, SURF also operates only on the model’s final linear layer, allowing its linear surrogate to fully represent the model’s computation.

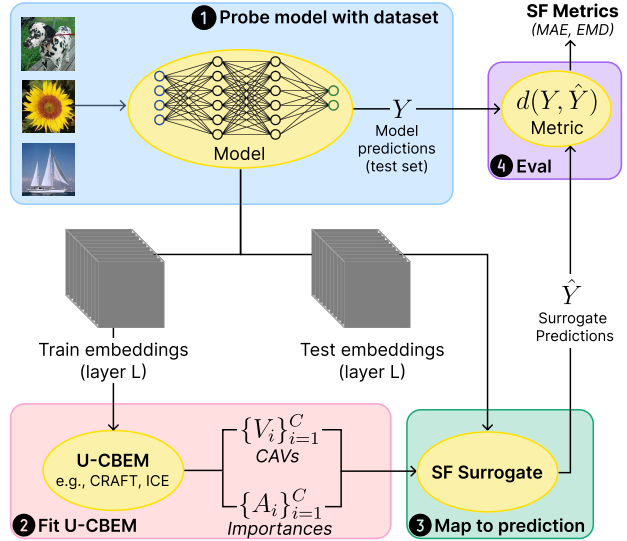


Figure 1. **Surrogate Faithfulness (SURF) overview.** (1) Probe the model with a dataset of inputs to obtain intermediate embeddings from the penultimate layer L . (2) A training subset of the embeddings is used to fit the U-CBEM, discovering CAVs and concept importances for all classes C . (3) A test set of embeddings (along with the learned U-CBEM parameters) are passed to the surrogate to be mapped to predictions. (4) The SURF metrics compare surrogate and model outputs to measure faithfulness.

5.2. The SURF Metrics

The SURF metrics measure the difference in model and surrogate outputs (Fig. 1, Step 4). For classification models, this means the logits. However, a model’s logit-space is unconstrained, varying drastically between models. This makes logit-space metrics difficult to interpret. Furthermore, metrics in the logit-space dilute the importance of the predicted class by aggregating errors over all classes. On the other hand, the probability-space (after softmax) normalizes the logits, allowing for a bounded, interpretable metric. However, low error in the probability-space *does not* always imply low error in the logit-space. Due to the softmax, the probability-space emphasizes the predicted class and diminishes the other classes, so one could achieve a low error by accurately reproducing the predicted class and ignoring the others. Since each space addresses the other’s flaws, SURF measures errors in both spaces.

Let ϕ be a classification model, where $\mathbf{y} \in \mathbb{R}^C$ denotes class logits. **To measure errors in the logit-space**, we use the mean absolute error (MAE) between the logits:

$$MAE = \frac{1}{|\mathcal{V}|C} \sum_{\mathbf{x} \in \mathcal{V}} \sum_{i=1}^C |y_i - \hat{y}_i| \quad (11)$$

where \mathcal{V} is the set of inputs used to evaluate for faithfulness. **To measure errors in the probability-space**, we find the

Table 3. **Measure-over-measure comparison.** We compare surrogate-based measures across three explanation settings (*Perfect*, *Rand Imp*, and *Full Rand*). We expect evaluations in the *Perfect* setting to give perfect faithfulness scores, and we expect progressively worse faithfulness evaluations as we increase randomness (just importances in *Rand Imp* and fully random in *Full Rand*). We include the SURF metrics (MAE and EMD) along with other metrics used by prior works. The SURF measure behaves as expected, whereas C-SHAP-Eval reports higher faithfulness in the *Full Rand* setting and ICE-Eval reports perfect faithfulness scores in the *Rand Imp* setting.

	Surrogate	Top-1 (%)	Rank Corr	Norm L1	MAE	EMD	Learnable Params.
Perfect	C-SHAP-Eval (CEL)	9.06	-0.18	0.94	1.72	0.842	1M
	C-SHAP-Eval (L1)	0.51	0.44	1.34	0.86	0.846	1M
	ICE-Eval	100	1.00	0.00	0.00	0.000	0
	SF (Ours)	100	1.00	0.00	0.00	0.000	0
Rand Imp	C-SHAP-Eval (CEL)	9.06	-0.18	0.94	1.72	0.842	1M
	C-SHAP-Eval (L1)	0.51	0.44	1.34	0.86	0.846	1M
	ICE-Eval	100	1.00	0.00	0.00	0.000	0
	SF (Ours)	76.7	0.60	0.43	0.72	0.380	0
Full Rand	C-SHAP-Eval (CEL)	86.9	0.42	12.2	14.9	0.249	1M
	C-SHAP-Eval (L1)	7.7	0.53	1.29	0.729	0.853	1M
	ICE-Eval	3.4	0.07	1.00	1.66	0.862	0
	SF (Ours)	1.2	-0.01	1.00	1.70	0.864	0

Earth Mover’s Distance (EMD) using a constant distance cost. Letting $\mathbf{p} \in \mathbb{R}^C$ denote class probability scores,

$$EMD = \frac{1}{2|\mathcal{V}|} \sum_{\mathbf{x} \in \mathcal{V}} \sum_{i=1}^C |p_i - \hat{p}_i| \quad (12)$$

For a U-CBEM to be faithful, its explanations must have low EMD and MAE errors. For regression, we only use MAE.

In contrast to prior surrogate-based approaches, Surrogate Faithfulness (SURF) meets all of our desiderata. (1) It introduces a simple surrogate with no additional learnable parameters: the output for any class i is a linear combination of the concept basis, weighted by the concept importances (A_i). The surrogate is *not reconstruction-based*; it tries to predict the **next** linear representation (e.g., class logits), instead of reconstructing embedding \mathbf{h} . Thus, only concepts useful for the prediction are needed, which may only be a subset of the concepts needed for reconstructing \mathbf{h} from $\mathcal{P}(\mathbf{h}; V)$. (2) SURF’s surrogate incorporates A_i , allowing inaccuracies in A_i to affect faithfulness scores. (3) SURF defines two metrics d that measure errors across the entire output space, instead of specific classes, to comprehensively assess faithfulness. These differences are summarized in Tab. 2.

6. Experiments

We perform experiments to: (1) empirically prove that SURF is a better faithfulness measure than prior ones; (2) benchmark prior U-CBEMs using SURF across three tasks, finding that many state-of-the-art U-CBEMs have poor faithfulness; (3) analyze the impact of the number

of concepts on faithfulness; (4) study the robustness of U-CBEMs in adversarial settings, a novel scenario that has been unexplored in prior evaluations.

6.1. Measure-over-Measure Comparison

We validate SURF against ICE-Eval and C-SHAP-Eval. As there is no “groundtruth” of faithfulness to compare evaluation results to, we test the frameworks in three manufactured settings, where we know the relative faithfulness of the explanations a priori. Specifically, we look at faithfulness results for a *perfect* explanation and two *randomized* explanations. To generate the *Perfect* explanation, observe that the most faithful explanation of the model is the model itself. Thus, we set $\{A_i, V_i\}_{i=1}^C$ according to the weights of the linear classification layer. In our second setting (termed *Rand Imp*), we keep the perfect CAVs fixed and randomly sample the concept importances. Our final setting (termed *Full Rand*) additionally randomly samples the CAVs. In the *Perfect* setting, we expect to obtain no faithfulness error, regardless of the evaluation measure. Then, we expect to obtain increasingly less faithful scores as we progressively increase randomness (from *Rand Imp* to *Full Rand*).

We evaluate the faithfulness in these three settings on an ImageNet-pretrained ResNet-50 [16] finetuned on the Caltech-101 dataset [21]. Along with the SURF metrics, we report ICE’s Top-1 Accuracy (**Top-1**) defined in Eq. (6) and ICE’s normalized L1 logit error (**Norm L1**) defined in Eq. (5). As a complementary measure to EMD, we measure Spearman’s rank correlation (**Rank Corr**) between surrogate and model outputs. This measure ensures that fine-grained changes that result in a different prediction ordering are penalized but ignores differences in magnitudes. Fi-

Table 4. **Benchmarking U-CBEM faithfulness.** We apply SURF to evaluate explanations from prior U-CBEMs in three tasks. Along with the SURF metrics (MAE and EMD), we report other metrics to serve as a comparison. We find that most prior U-CBEMs are not faithful, as indicated by large errors in the logit and probability space.

(a) Object classification (ResNet-50)					(b) Multi-attribute prediction (MobileNetV2)		(c) Age (ViT)
U-CBEM	MAE (↓)	EMD (↓)	Top-1 (%) (↑)	Rank Corr (↑)	MAE (↓)	Attr-Acc (%) (↑)	MAE (↓)
CDISCO	2.29	0.957	0.9	0.000	6.77	50.7	32.6
ICE	3.06	<u>0.438</u>	<u>93.1</u>	0.222	<u>5.55</u>	<u>76.1</u>	-
CRAFT	<u>1.70</u>	0.844	78.9	<u>0.484</u>	6.87	19.6	-
C-SHAP	2.40	0.587	41.7	0.461	7.75	51.0	-
MCD	1.42	0.079	97.0	0.808	2.83	96.6	-

nally, we measure surrogate complexity with the number of learnable parameters the evaluation measure introduces. Since C-SHAP-Eval’s two-layer perceptron was originally trained with cross entropy loss (CEL), we also train the surrogate with L1 loss, as this may align better with the SURF metrics. More details in Appendix Sec. A.

Results are reported in Tab. 3, averaged over 10 seeds. In the *Perfect* setting, both ICE-Eval and SURF report perfect faithfulness, as expected. However, both C-SHAP-Eval variants are unable to achieve perfect faithfulness across any metric, showing C-SHAP-Eval’s limitations. In the *Rand Imp* setting, we observe that C-SHAP-Eval and ICE-Eval do not report differences when compared to the *Perfect* setting; this occurs because they do not use concept importances, so even random concept importances have the same result as the *Perfect* setting. Contrast this with SURF, which clearly finds a deterioration in faithfulness across *all* metrics. Finally, in the *Full Rand* setting, C-SHAP-Eval unintuitively reports an improvement in faithfulness compared to the *Perfect* setting. ICE-Eval and SURF report similarly poor faithfulness scores for this setting, as expected. Of the tested faithfulness measures, SURF is the only one that behaves as expected, as validated by all metrics.

Next, we turn our attention to the metrics. We highlight a failure case of Top-1 by looking at C-SHAP-Eval (CEL)’s results in the *Full Rand* setting. The Top-1 score is strong; however, the other metrics (especially EMD) reveal that the reconstructed output has severe errors on the remainder of the output distribution. Norm L1 also comes with issues; notice how C-SHAP-Eval (CEL) reports a lower error compared to C-SHAP-Eval (L1), despite C-SHAP-Eval (L1) directly minimizing the L1 error between logits. We attribute this inconsistency to Norm L1’s emphasis on *only the groundtruth class*; while the L1 error across other classes (as measured by MAE) has decreased, the normalized error for the *groundtruth class* increased, giving an incomplete picture of faithfulness.

As shown in the three settings presented, SURF is able to appropriately measure the faithfulness of three toy U-CBEMs. This contrasts with other approaches and metrics,

which fail to yield satisfactory measurements in the same three cases. The remainder of the paper uses SURF to evaluate prior U-CBEMs.

6.2. Benchmarking U-CBEMs

We evaluate five prior U-CBEMs (CDISCO, ICE, CRAFT, C-SHAP, and MCD). We benchmark U-CBEMs on a varied range of tasks with a diverse range of models to demonstrate the applicability of SURF. Specifically, our tasks are: 1) *Object Classification*, 2) *Multi-Attribute Prediction*, and 3) *Age Regression*. In all tasks, each U-CBEM discovers 5 CAVs (or subspaces for MCD) per output. CAVs and importances are found on the training set, and the resulting explanations are evaluated on the test set. Dataset, finetuning, and U-CBEM implementation details are in Sec. B. Good-faith efforts were made to adapt prior U-CBEMs (that were developed for object classification) to new tasks.

We evaluate on three tasks. **(1) Object Classification:** We finetune a ResNet-50 on Caltech-101 and report MAE, EMD, Top-1, and Rank Corr. **(2) Multi-Attribute Prediction:** Given an image, we finetune a MobileNetV2 [31] to predict the presence/absence of attributes in the CelebA dataset [22]. We report MAE and attribute prediction accuracy (Attr-Acc), which is introduced as a task-specific replacement for Top-1. **(3) Age Estimation:** Given a human face, we finetune a ViT [6] to predict their age (in years) on the UTK-Face dataset [45]. Because ViTs have negative activations, U-CBEMs with non-negativity assumptions (i.e., ICE and CRAFT) cannot be used. C-SHAP is omitted as it is only applicable to classification, and MCD is incompatible with ViTs. For this task, we report MAE.

Benchmark results are reported in Tab. 4. Aside from MCD, we observe that **no prior U-CBEM is faithful to the original model**, on any task. In the *Object Classification* task, the most faithful U-CBEM (after MCD) achieves the lowest EMD of 0.438, denoting large errors in the probability-space which stem from errors in the logit-space. Only two of the tested U-CBEMs (ICE and MCD) perform significantly above random chance in the *Multi-Attribute Prediction* task. CDISCO exhibits an average error of 32.6

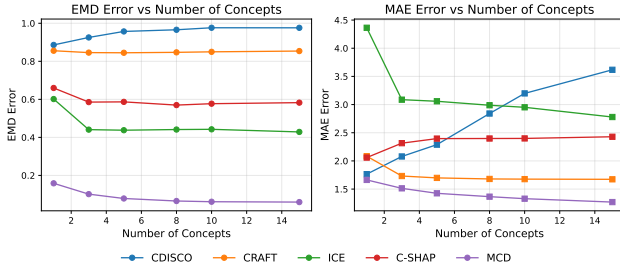


Figure 2. We fit U-CBEMs on Sec. 6.2’s *Object Classification* task with an increasing number of concepts and evaluate them with SURF. Some U-CBEMs do not improve as the number of concepts increase. U-CBEMs that improve quickly plateau, indicating an “elbow” phenomenon.

years in the *Age Estimation* task.

We believe that U-CBEMs are unfaithful for two reasons: (1) Other than C-SHAP, all methods discover class-specific CAVs to reconstruct the embedding. Crucially, the class-specific CAVs are found on images from *only* that class, so using class c_1 ’s CAVs to reconstruct an embedding from an image of class c_2 will result in large reconstruction error (e.g., the U-CBEM is operating out-of-distribution), and therefore, large logit- and probability-space errors. This issue is exacerbated for CRAFT & ICE, which non-linearly project to the concept space. (2) Except for ICE and MCD, the concept importance scores do not satisfy a logit-based completeness criterion (note, C-SHAP satisfies an accuracy-based completeness criterion). Thus, the concept importances do not faithfully reflect the impact of the concept representation on the model’s outputs. Though MCD also finds class-specific concepts, MCD achieves superior faithfulness by allowing a concept to be the span of many CAVs (a linear subspace); thus, it is able to faithfully explain a larger part of the model’s reasoning with the same number of concepts.

6.3. Faithfulness vs. Parsimony

The *most important hyperparameter* for any U-CBEM is the number of concepts to be discovered. Intuitively, having more concepts should result in a more complete (i.e., faithful) explanation. However, presenting users with explanations containing too many concepts may be uninterpretable. The cognitive psychology literature has shown that humans can hold a limited number of items in their working memory at a time [5, 25]. Thus, simple, or *parsimonious*, explanations are preferred, which can communicate the bulk of the model’s reasoning in a few concepts. Instead of setting this hyperparameter arbitrarily, something commonly done in prior U-CBEMs (10 in [44], 25 in [9, 13]), we use SURF to intelligently analyze this tradeoff.

Using the *Object Classification* task from Sec. 6.2, we fit

Table 5. **Novel setting: faithfulness on adversarial images.** U-CBEMs are **fixed** from Sec. 6.2’s *Object Classification* task. The original model is adversarially attacked, and we report the mean paired difference in MAE and EMD (adversary – original) on 100 randomly sampled images. Any statistically insignificant difference is omitted (with “-”). U-CBEMs are generally not robust to adversarial attack; all of them exhibit an increase in MAE.

U-CBEM	MAE (↓)	EMD (↓)
CDISCO	+0.634	+0.039
ICE	+0.730	-
CRAFT	+0.411	+0.073
C-SHAP	+0.631	-0.195
MCD	+0.339	-0.038

U-CBEMs with an increasing number of concepts. Each U-CBEM is evaluated using the SURF measure, visualized in Fig. 2. We observe that some U-CBEMs (CDISCO, CRAFT, C-SHAP) either do not improve or perform worse on one or both metrics as they discover more concepts. Only ICE and MCD uniformly improve as the number of concepts increases, and they exhibit an “elbow” phenomenon, marking a natural choice for the number of concepts.

6.4. Faithfulness in Adversarial Settings

Prior work has restricted their faithfulness evaluations to explanations on images from the *same* dataset the U-CBEM was trained on, as we did in Sec. 6.2. Such evaluations do not test U-CBEMs in challenging situations; yet, we believe these situations are the ones where having faithful explanations *are the most critical*. One such scenario is adversarial attack, which we test here. We take on the role of an adversary who has white-box access to the original model, but is unaware of the post-hoc explanation. If the U-CBEM is robust to adversarial attack, then we expect the U-CBEM to faithfully explain the model when it is under adversarial attack, allowing stakeholders to be aware of the adversarial attack. We design a Projected Gradient Descent (PGD) attack [24] to maximize the probability distribution difference of the original model on the input image and the adversary (details in Appendix Sec. C). The PGD attack is repeated on a 100 randomly sampled images from the training set for U-CBEMs fit in the *Object Classification* task from Sec. 6.2.

Tab. 5 reports the mean paired difference in MAE and EMD (adversarial – original). We use a one-sided, paired t-test on per-image differences to determine statistically significant increases in error (if $p < 0.01$). We find that the MAE error increase is significant for all U-CBEMs, while EMD only significantly increases for CDISCO and CRAFT. We conclude that all U-CBEMs are less robust in the logit space, with ICE being the most vulnerable. The logit-space errors only propagate to the probability space for certain U-CBEMs (CDISCO & CRAFT). In certain cases (e.g., C-

SHAP), the probability-space error may actually decrease on adversarial examples. We anticipate that U-CBEMs may be more vulnerable to adversarial attacks specifically designed to fool the explainer (instead of the model); as demonstrated under a simple PGD attack, SURF makes it possible to study such scenarios.

7. Conclusion

This paper organizes prior faithfulness measures, discusses their limitations, and proposes SURF to accurately measure faithfulness. We validate SURF compared to other measures in a measure-over-measure study, and we use SURF to find that several existing U-CBEMs produce unfaithful explanations. We apply SURF to downstream settings (number of concepts selection and adversarial robustness) to demonstrate its utility. We urge future works to adopt SURF to comprehensively evaluate faithfulness and compare to prior works.

References

- [1] Julius Adebayo, Justin Gilmer, Michael Muelly, Ian J. Goodfellow, Moritz Hardt, and Been Kim. Sanity checks for saliency maps. In *Adv. Neural Inform. Process. Syst.*, 2018. 1
- [2] Zeynep Akata, Ulrike von Luxburg, Uddeshya Upadhyay, and Sebastian Bordt. The manifold hypothesis for gradient-based explanations. In *IEEE Conf. Comput. Vis. Pattern Recog. Worksh.*, 2022. 4
- [3] David Bau, Bolei Zhou, Aditya Khosla, Aude Oliva, and Antonio Torralba. Network dissection: Quantifying interpretability of deep visual representations. *IEEE Conf. Comput. Vis. Pattern Recog.*, pages 3319–3327, 2017. 1
- [4] Julien Colin, Thomas Fel, Remi Cadene, and Thomas Serre. What i cannot predict, i do not understand: A human-centered evaluation framework for explainability methods. In *Adv. Neural Inform. Process. Syst.*, 2022. 1
- [5] Nelson Cowan. The magical mystery four. *Current Directions in Psychological Science*, 19:51 – 57, 2010. 8
- [6] Alexey Dosovitskiy, Lucas Beyer, Alexander Kolesnikov, Dirk Weissenborn, Xiaohua Zhai, Thomas Unterthiner, Mostafa Dehghani, Matthias Minderer, Georg Heigold, Sylvain Gelly, Jakob Uszkoreit, and Neil Houlsby. An image is worth 16x16 words: Transformers for image recognition at scale. In *Int. Conf. Learn. Represent.*, 2021. 7
- [7] Thomas FEL, Remi Cadene, Mathieu Chalvidal, Matthieu Cord, David Vigouroux, and Thomas Serre. Look at the variance! efficient black-box explanations with sobol-based sensitivity analysis. In *Adv. Neural Inform. Process. Syst.*, 2021. 1
- [8] Thomas Fel, Lucas Hervier, David Vigouroux, Antonin Poche, Justin Plakoo, Remi Cadene, Mathieu Chalvidal, Julien Colin, Thibaut Boissin, Louis Bethune, Agustin Picard, Claire Nicodeme, Laurent Gardes, Gregory Flandin, and Thomas Serre. Xplique: A deep learning explainability toolbox. *Workshop on Explainable Artificial Intelligence for Computer Vision (CVPR)*, 2022. 2
- [9] Thomas Fel, Agustin Picard, Louis Béthune, Thibaut Boissin, David Vigouroux, Julien Colin, Rémi Cadène, and Thomas Serre. Craft: Concept recursive activation factorization for explainability. *IEEE Conf. Comput. Vis. Pattern Recog.*, pages 2711–2721, 2022. 2, 3, 8
- [10] Ruth Fong and Andrea Vedaldi. Net2vec: Quantifying and explaining how concepts are encoded by filters in deep neural networks. *IEEE Conf. Comput. Vis. Pattern Recog.*, pages 8730–8738, 2018. 1
- [11] Christopher Frye, Damien de Mijolla, Laurence Cowton, Megan Stanley, and Ilya Feige. Shapley-based explainability on the data manifold. *Int. Conf. Learn. Represent.*, abs/2006.01272, 2021. 1, 4
- [12] Julie Gerlings, Arisa Shollo, and Ioanna D. Constantiou. Re-viewing the need for explainable artificial intelligence (xai). In *Hawaii Int. Conf. on System Sciences*, 2020. 1
- [13] Amirata Ghorbani, James Wexler, James Y. Zou, and Been Kim. Towards automatic concept-based explanations. In *Adv. Neural Inform. Process. Syst.*, 2019. 2, 3, 8
- [14] Mara Graziani, An phi Nguyen, Laura O’Mahony, Henning Müller, and Vincent Andearczyk. Concept discovery and dataset exploration with singular value decomposition. In *ICLR 2023 Workshop on Pitfalls of limited data and computation for Trustworthy ML*, 2023. 2, 3
- [15] Peter Hase, Harry Xie, and Mohit Bansal. The out-of-distribution problem in explainability and search methods for feature importance explanations. In *Adv. Neural Inform. Process. Syst.*, 2021. 1, 4
- [16] Kaiming He, X. Zhang, Shaoqing Ren, and Jian Sun. Deep residual learning for image recognition. *IEEE Conf. Comput. Vis. Pattern Recog.*, pages 770–778, 2016. 6
- [17] Been Kim, Martin Wattenberg, Justin Gilmer, Carrie J. Cai, James Wexler, Fernanda B. Viégas, and Rory Sayres. Interpretability beyond feature attribution: Quantitative testing with concept activation vectors (tcav). In *Int. Conf. Machine Learn.*, 2017. 1, 2
- [18] Eunji Kim, Dahuin Jung, Sangha Park, Siwon Kim, and Sung-Hoon Yoon. Probabilistic concept bottleneck models. In *International Conference on Machine Learning*, 2023. 3
- [19] Diederik P Kingma. Adam: A method for stochastic optimization. In *Int. Conf. Learn. Represent.*, 2015. 1
- [20] Pang Wei Koh, Thao Nguyen, Yew Siang Tang, Stephen Mussmann, Emma Pierson, Been Kim, and Percy Liang. Concept bottleneck models. In *Proceedings of the 37th International Conference on Machine Learning*, pages 5338–5348. PMLR, 2020. 3
- [21] Fei-Fei Li, Marco Andreetto, Marc’Aurelio Ranzato, and Pietro Perona. Caltech 101, 2022. 6
- [22] Ziwei Liu, Ping Luo, Xiaogang Wang, and Xiaoou Tang. Deep learning face attributes in the wild. In *Proceedings of International Conference on Computer Vision (ICCV)*, 2015. 7
- [23] Scott M. Lundberg and Su-In Lee. A unified approach to interpreting model predictions. In *Adv. Neural Inform. Process. Syst.*, 2017. 1, 3
- [24] Aleksander Madry, Aleksandar Makelov, Ludwig Schmidt, Dimitris Tsipras, and Adrian Vladu. Towards deep learning

models resistant to adversarial attacks. In *Int. Conf. Learn. Represent.*, 2018. 8, 3

[25] George A. Miller. The magical number seven plus or minus two: some limits on our capacity for processing information. *Psychological review*, 63(2):81–97, 1956. 8

[26] Giang Nguyen, Daeyoung Kim, and Anh Totti Nguyen. The effectiveness of feature attribution methods and its correlation with automatic evaluation scores. In *Adv. Neural Inform. Process. Syst.*, 2021. 1

[27] Tuomas Oikarinen, Subhro Das, Lam M Nguyen, and Tsui-Wei Weng. Label-free concept bottleneck models. In *International Conference on Learning Representations*, 2023. 3

[28] Vitali Petsiuk, Abir Das, and Kate Saenko. Rise: Randomized input sampling for explanation of black-box models. In *Proceedings of the British Machine Vision Conference (BMVC)*, 2018. 1

[29] Vikram V. Ramaswamy, Sunnie S. Y. Kim, Ruth C. Fong, and Olga Russakovsky. Overlooked factors in concept-based explanations: Dataset choice, concept learnability, and human capability. *IEEE Conf. Comput. Vis. Pattern Recog.*, pages 10932–10941, 2023. 1

[30] Marco Tulio Ribeiro, Sameer Singh, and Carlos Guestrin. “why should i trust you?”: Explaining the predictions of any classifier. *Proc. of the 22nd ACM SIGKDD Int. Conf. on Knowledge Discovery and Data Mining*, 2016. 1, 2

[31] Mark Sandler, Andrew G. Howard, Menglong Zhu, Andrey Zhmoginov, and Liang-Chieh Chen. Mobilenetv2: Inverted residuals and linear bottlenecks. *2018 IEEE/CVF Conference on Computer Vision and Pattern Recognition*, pages 4510–4520, 2018. 7

[32] Leon Sixt, Maximilian Granz, and Tim Landgraf. When explanations lie: Why many modified bp attributions fail. In *Int. Conf. Machine Learn.*, 2020. 1

[33] Dylan Slack, Sophie Hilgard, Emily Jia, Sameer Singh, and Himabindu Lakkaraju. Fooling lime and shap: Adversarial attacks on post hoc explanation methods. In *AAAI/ACM Conference on AI, Ethics, and Society (AIES)*, 2020. 4

[34] Muhammad Faaiz Taufiq, Patrick Blöbaum, and Lenon Minornics. Manifold restricted interventional shapley values. In *Int. Conf. on Artificial Intelligence and Statistics*, pages 5079–5106. PMLR, 2023. 4

[35] Johanna Vielhaben, Stefan Bluecher, and Nils Strodthoff. Multi-dimensional concept discovery (MCD): A unifying framework with completeness guarantees. *Transactions on Machine Learning Research*, 2023. 2, 3

[36] Minh N Vu, Huy Q Mai, and My T Thai. Emap: Explainable ai with manifold-based perturbations. *arXiv preprint arXiv:2209.08453*, 2022. 4

[37] Jianyu Wang, Zhishuai Zhang, Cihang Xie, Vittal Premachandran, and Alan Loddon Yuille. Unsupervised learning of object semantic parts from internal states of cnns by population encoding. *arXiv: Learning*, 2015. 2

[38] Yongjie Wang, Tong Zhang, Xu Guo, and Zhiqi Shen. Gradient based feature attribution in explainable ai: A technical review. *arXiv preprint arXiv:2403.10415*, 2024. 1

[39] Chih-Kuan Yeh, Been Kim, Sercan Ö. Arik, Chun-Liang Li, Tomas Pfister, and Pradeep Ravikumar. On completeness-aware concept-based explanations in deep neural networks. *Adv. Neural Inform. Process. Syst.*, 2020. 2, 1

[40] Chih-Kuan Yeh, Kuan-Yun Lee, Frederick Liu, and Pradeep Ravikumar. Threading the needle of on and off-manifold value functions for shapley explanations. In *Int. Conf. on Artificial Intelligence and Statistics*, pages 1485–1502. PMLR, 2022. 4

[41] H. Peyton Young. Monotonic solutions of cooperative games. *International Journal of Game Theory*, 14:65–72, 1985. 2

[42] Mert Yuksekgonul, Maggie Wang, and James Zou. Post-hoc concept bottleneck models. In *The Eleventh International Conference on Learning Representations*, 2023. 3

[43] Eslam Zaher, Maciej Trzaskowski, Quan Nguyen, and Fred Roosta. Manifold integrated gradients: Riemannian geometry for feature attribution. *Int. Conf. Machine Learn.*, 2024. 4

[44] Ruihan Zhang, Prashan Madumal, Tim Miller, Krista A. Ehinger, and Benjamin I. P. Rubinstein. Invertible concept-based explanations for cnn models with non-negative concept activation vectors. In *AAAI*, 2020. 2, 8

[45] Zhifei Zhang, Yang Song, and Hairong Qi. Age progression/regression by conditional adversarial autoencoder. In *IEEE Conference on Computer Vision and Pattern Recognition (CVPR)*. IEEE, 2017. 7

[46] Bolei Zhou, Aditya Khosla, Agata Lapedriza, Aude Oliva, and Antonio Torralba. Object detectors emerge in deep scene cnns. *Int. Conf. Learn. Represent.*, 2015. 1

Measuring the (Un)Faithfulness of Concept-Based Explanations

Supplementary Material

This supplementary section provides information not included in the main text due to space constraints. It includes:

1. Sec. A: Implementation details for the surrogate justification experiment (Sec. 6.1).
2. Sec. B: Experimental details for the evaluation of U-CBEMs done in Sec. 6.2.
3. Sec. C: Experimental details for the adversarial attack experiment done in Sec. 6.4.

A. Implementation Details for Measure-over-Measure Comparison

This section contains details for the measure-over-measure comparison conducted in Sec. 6.1.

A.1. Experimental Setting Details

In the *Perfect* setting, we set CAVs and importances according to the weights of the final classification layer. Specifically, each class has 1 CAV ($K = 1$). The CAV $\mathbf{v}_{c,1}$ for class c is set to $\frac{\mathbf{f}_c}{\|\mathbf{f}_c\|_2}$, where \mathbf{f}_c is class c 's classification vector. The CAV's importance $\alpha_{c,1}$ is set to $\|\mathbf{f}_c\|_2$.

For the *random* settings, we sample each dimension of the CAVs independently from a standard normal distribution, and then make the CAV unit norm. We sample concept importances uniformly from $[0, 1]$.

A.2. Surrogate Implementation

Recall that U-CBEMs define their own mechanism $\mathcal{P} : \mathcal{H} \rightarrow \mathbb{R}^K$ to project embeddings to the concept basis. For these experiments, since we are not using any U-CBEM and instead directly setting the CAVs and importances, we define $\mathcal{P}(\mathbf{h}_j, V_i)_k = \mathbf{h}_j^T \mathbf{v}_{i,k}$, where i denotes the class, k denotes the CAV, and j selects the spatial embedding. Recall in this case that $K = 1$ and there is only one embedding (obtained from global pooling).

A.2.1. SF Surrogate (Ours)

Following Sec. 5.1 and Eq. (10), we set the parameters of the surrogate with the concepts and importances obtained from the setting. This surrogate has no learnable parameters and is exactly equal to the original linear. Note that the embeddings are linearly projected onto the CAVs to find the concept representation.

A.2.2. ICE Surrogate

ICE's surrogate takes the concept representation and reconstructs the embedding, as specified by the U-CBEM. It then passes through the final classification layer to obtain outputs. Let $\mathbf{p}_i \in \mathbb{R}^K$ denote the concept representation for

class i obtained from embedding \mathbf{h} . The surrogate is:

$$y_i = \mathbf{f}_i^T \psi_{ICE}(\mathbf{p}_i) + b_i \quad (13)$$

where $\psi_{ICE}(\cdot)$ denotes the reconstruction, as specified by the U-CBEM. Since we are not making use of any U-CBEM in the measure-over-measure comparison, we use linear operations to reconstruct the embedding from the concept representation. That is, $\psi(\mathbf{p}_i) = \sum_{k=1}^K p_{i,k} \mathbf{v}_{i,k}$.

A.2.3. C-SHAP Surrogate

C-SHAP's surrogate defines a two-layer MLP $\psi_{C-SHAP}(\cdot)$ to reconstruct the embedding, and then passes through the final classification layer to obtain outputs. The surrogate is:

$$y_i = \mathbf{f}_i^T \psi_{C-SHAP}(\mathbf{p}_i) + b_i \quad (14)$$

Since C-SHAP's surrogate contains learnable parameters. Following [39], the MLP's hidden layer has a dimensionality of 500, and the surrogate is trained using Cross Entropy Loss between the surrogate's predicted class probabilities and the original model's class probabilities. We train the surrogate using the Adam optimizer [19] and a starting learning rate of 0.1. The surrogate is trained for at most 100 epochs, during which the learning rate is decayed by a factor of 0.5 when the training loss plateaus. We stop training when the learning rate is reduced below 10^{-7} .

B. Additional Details for Benchmarking U-CBEM Faithfulness

Sec. 6.2 evaluates prior U-CBEMs, finding that they produce unfaithful explanations. This section gives experimental and implementation details for this evaluation.

B.1. Model Details

Object Classification: Our evaluation uses a ResNet-50. We use the ImageNet pre-trained weights and initialize the final classification layer with random weights. The model is finetuned (conv4 and all subsequent layers) on the Caltech-101 training set, achieving a test accuracy of approximately 92.75%. The model is trained without data augmentation and using cross entropy loss.

Multi-Attribute Prediction: We finetune an ImageNet pre-trained MobileNetV2 on the CelebA dataset for the task of binary attribute prediction. We initialize the final prediction linear layer with random weights, and finetune all layers of the model. We achieve an attribute prediction accuracy of 91.55%. The model is trained with data augmentation and binary cross-entropy loss.

Age Regression: We finetune an ImageNet pre-trained Vision Transformer (ViT) on the UTK-Face dataset for the task of age regression. We choose the ViT-B/16 variant for our experiment. We initialize the final prediction linear layer with random weights, and finetune all weights above (not including) the 9th layer. The model achieves a mean average error of 5.14 on the test set. The model is trained with data augmentation and using L1 Loss.

B.2. Dataset Details

We learn each class’s concepts and importances using images of the class from the training set. Importantly, the label of each image is determined using the original model’s prediction (instead of the ground truth label). We do this because we are interested in explaining why *the model* predicts a specific label, regardless of whether the prediction is correct or not. After learning the U-CBEMs, we evaluate them on a test set.

Object Classification: We split Caltech-101’s dataset into train and test sets using 80/20 splits. While splitting the data, we maintain the same class distribution present in the original dataset in both the training and testing splits. To handle Caltech-101’s class imbalance, we assemble a balanced test set; this ensures that we evaluate for faithfulness equally across all classes.

Multi-Attribute Prediction: We use CelebA’s pre-defined train and test sets. We do not make any modifications to the test set. Since the training set is too large for many U-CBEMs, we take a random subset of training data to use for finding U-CBEM parameters. The random subset is equivalent in size to the test set.

Age Regression: We split the dataset into train and test sets using 80/20 splits. While splitting the data, we discretize the age distribution into bins of 10-years, and maintain this distribution across both the training and testing splits. As UTK-Face does not have any classes, all U-CBEMs find CAVs on all embeddings.

B.3. U-CBEM Details

This section specifies implementation details for each U-CBEM that was benchmarked.

B.4. CDISCO

The open-source implementation provided by the authors was used to evaluate this approach. CDISCO uses SVD to discover CAVs. Then, a gradient-based approach is used to calculate the importance of each CAV. The code used to compute the gradients was not provided in the repository, so we re-implemented it. Embeddings are linearly projected to the concept space.

Object Classification: Due to a lack of clarity, we had to make one implementation choice. Specifically, when finding the importance (using a gradient calculation), it was un-

clear if we should use images from all classes or only images of the CAV’s class. We opted for the latter, based on the code and the example provided by the authors.

Multi-Attribute Prediction: CDISCO was extended to this task by reformulating the task as independent binary classification tasks. Thus, CAVs and concept importances were learned for each task independently

Age Regression: The open-source implementation only considered the case of multi-class classification. According to the paper and the code used for multi-class classification, we re-implemented CDISCO to work in the case of single-output regression.

B.5. ICE

The open-source implementation provided by the authors was used to evaluate this approach. ICE uses NMF to find CAVs. Due to the potentially large number of embeddings, we use the batched-version of NMF. Concept importance is found using the TCAV method proposed in [17]. Embeddings are projected to the concept space using sci-kit learn’s transform method. ICE was extended to multi-attribute prediction by reformulating the task as independent binary classification tasks. Thus, CAVs and concept importances were learned for each task independently.

B.6. CRAFT

The open-source implementation provided in the Xplique toolbox [8] (by the same authors) was used to evaluate this approach. CRAFT uses NMF to find CAVs and introduces a Sobol-based sensitivity approach to find concept importance. Embeddings are projected to the concept space using the toolbox’s built-in transform method.

B.7. ConceptSHAP

ConceptSHAP differs from previous U-CBEMs because it discovers CAVs globally (i.e., class-agnostic). Thus, we need a way to associate discovered CAVs to the concepts. To do so, we discover a (larger than K) set of CAVs and assign them a per-class concept importance score (through Shapley Values). Then, the top K CAVs by importance magnitude are selected to be the CAVs for a given class. For all experiments, we initially discover 100 CAVs. This number is arbitrary, but note that the Shapley Value computation scales exponentially with the number of initially discovered CAVs, which motivated our choice. With more CAVs, we expect ConceptSHAP to obtain higher faithfulness at the expense of a higher computational cost. Embeddings are linearly projected to the concept space. For age regression, we only discover K concepts (since there are no classes). For multi-attribute prediction, we repeat the ConceptSHAP procedure for each attribute, considering each attribute prediction as a binary classification task; we only discover K concepts, since each task is a binary classification.

The authors provide an open-source implementation in TensorFlow, so we instead use a [third-party re-implementation](#) in PyTorch. Several modifications are made to this implementation:

1. Added in a learnable two-layer MLP to map back to the representation space (as done in the original paper)
2. Added more efficient concept importance scoring via Shapley Values. This is implemented using KernelSHAP ([23]) and is class-specific.
3. Fixed the implementation of the completeness score

B.8. MCD

Instead of representing concepts as single CAVs, MCD represents concepts as multi-dimensional subspaces. In [35], any concept l for class i is characterized by a representative basis $C^{i,l} = \{\mathbf{v}_j^{i,l} | j = 1 \dots d_l\}$, where d_l denotes the dimensionality of the subspace. To ensure the union of all concepts span the entire feature space, they define the orthogonal complement concept $C^{i,\perp} = \text{span}(C^{i,1}, \dots, C^{i,K})^\perp$, where K is the number of concepts originally discovered, letting $C^{i,K+1} \equiv C^{i,\perp}$. Then, any embedding \mathbf{h} can be uniquely decomposed onto the concept basis as:

$$\mathbf{h} = \sum_{l=1}^{n_c+1} \sum_{j=1}^{d^l} p_j^{i,l} \mathbf{v}_j^{i,l} \quad (15)$$

Thus, we stack all $p_j^{i,l}$ into the concept representation \mathbf{p}_i for class i . Since $C^{i,\perp}$ is not interpretable, we set elements of \mathbf{p}_i corresponding to $C^{i,\perp}$ to 0; thus, the reconstruction of \mathbf{h} is done using interpretable concepts presented to the user during an explanation. We set concept importance $\alpha_j^{i,l} = \mathbf{f}_i^T \mathbf{v}_j^{i,l}$, which directly relates to the local and global concept relevance defined in MCD and allows for faithful reconstruction of the output using our surrogate.

Since MCD is computationally expensive when trying to discover concepts on a large number of embeddings, we randomly sample 10,000 embeddings if the number of embeddings extracted for a given class is above 10,000. We use the [open-source implementation](#) provided by the authors.

C. Adversarial Attack Details

We conducted a white-box adversarial attack using Projected Gradient Descent (PGD) [24] to evaluate the robustness of U-CBEMs under adversarial perturbations. The attack aims to maximize the EMD between the probability outputs of the model on the original image and the adversary.

A PGD attack with 100 iterations, step size $\alpha = 1$, and perturbation bound $\epsilon = 0.1$ was implemented to iteratively perturb input images while maximizing the EMD loss. The final perturbed image with the highest EMD loss (across all

iterations) was used for evaluation. The original implementation of PGD assumes that the images are normalized from [0,1] to define the perturbation bound. Our images were standardized (following typical ImageNet processing), so we empirically selected an ϵ that resulted in minor perceptible changes to the reference image.